

Article

Simulating Potential Impacts of Fuel Treatments on Fire Behavior and Evacuation Time of the 2018 Camp Fire in Northern California

Daisuke Seto ^{1,*}, Charles Jones ^{1,2}, Anna T. Trugman ^{1,2}, Kevin Varga ^{1,2}, Andrew J. Plantinga ³, Leila M. V. Carvalho ^{1,2}, Callum Thompson ¹, Jacob Gellman ³ and Kristofer Daum ^{1,2}

¹ Earth Research Institute, University of California, Santa Barbara, CA 93106, USA; cjones@eri.ucsb.edu (C.J.); att@ucsb.edu (A.T.T.); kvarga@ucsb.edu (K.V.); leila@eri.ucsb.edu (L.M.V.C.); callum@eri.ucsb.edu (C.T.); klddaum@ucsb.edu (K.D.)

² Department of Geography, University of California, Santa Barbara, CA 93106, USA

³ Bren School of Environmental Science and Management, University of California, Santa Barbara, CA 93106, USA; plantinga@bren.ucsb.edu (A.J.P.); gellman@ucsb.edu (J.G.)

* Correspondence: d_seto@ucsb.edu

Abstract: Fuel break effectiveness in wildland-urban interface (WUI) is not well understood during downslope wind-driven fires even though various fuel treatments are conducted across the western United States. The aim of this paper is to examine the efficacy of WUI fuel breaks under the influence of strong winds and dry fuels, using the 2018 Camp Fire as a case study. The operational fire growth model Prometheus was used to show: (1) downstream impacts of 200 m and 400 m wide WUI fuel breaks on fire behavior and evacuation time gain; (2) how the downstream fire behavior was affected by the width and fuel conditions of the WUI fuel breaks; and (3) the impacts of background wind speeds on the efficacy of WUI fuel breaks. Our results indicate that WUI fuel breaks may slow wildfire spread rates by dispersing the primary advancing fire front into multiple fronts of lower intensity on the downstream edge of the fuel break. However, fuel break width mattered. We found that the lateral fire spread and burned area were reduced downstream of the 400 m wide WUI fuel break more effectively than the 200 m fuel break. Further sensitivity tests showed that wind speed at the time of ignition influenced fire behavior and efficacy of management interventions.

Keywords: wildland-urban interface (WUI); fuels management; evacuation; Camp Fire; fuel break; fire spread modeling; fire intensity; rate of spread; downslope wind; Prometheus fire growth model



Citation: Seto, D.; Jones, C.; Trugman, A.T.; Varga, K.; Plantinga, A.J.; Carvalho, L.M.V.; Thompson, C.; Gellman, J.; Daum, K. Simulating Potential Impacts of Fuel Treatments on Fire Behavior and Evacuation Time of the 2018 Camp Fire in Northern California. *Fire* **2022**, *5*, 37. <https://doi.org/10.3390/fire5020037>

Academic Editors: Alistair Smith and James R. Meldrum

Received: 7 January 2022

Accepted: 5 March 2022

Published: 9 March 2022

Publisher's Note: MDPI stays neutral with regard to jurisdictional claims in published maps and institutional affiliations.



Copyright: © 2022 by the authors. Licensee MDPI, Basel, Switzerland. This article is an open access article distributed under the terms and conditions of the Creative Commons Attribution (CC BY) license (<https://creativecommons.org/licenses/by/4.0/>).

1. Introduction

Wildfire behavior regimes can be broadly characterized as either fuel-dominated or wind-dominated. These two wildfire regimes in California reflect differences in seasonal timing, ignition sources, and geographical distributions across the state, which is topographically, climatologically, and ecologically diverse [1]. Management responses need to consider this diversity to effectively mitigate fire risk. Fuel-dominated fires, also known as plume or convection-dominated fires [2–5], are predominantly controlled by anomalously high fuel loads and are common in central and northern California conifer forests during peak lightning season (June–July), coinciding with high air temperatures and low precipitation [6]. These fires tend to occur in low populated regions. The moderate rate of fire spread allows for easier community evacuation and fire suppression activities as a method for mitigating wildfire risk to human life and structures. Consequently, fuel-dominated fires usually do not result in significant loss of lives or properties. In contrast, wind-dominated fires are mostly caused by ignitions from humans or infrastructure failure, such as downed power lines during extreme downslope wind events. These are typically dry, warm, and gusty downslope windstorms occurring on the lee-side of mountain ranges and often have

geographically distinct names, such as the North, Diablo, Sundowner, and Santa Ana winds in California [7]. Large, fast-moving wildfires associated with these strong winds have long been recognized as costly and difficult to mitigate and control [8]. As population growth expands the wildland urban interface (WUI) into areas of higher wildfire risk, the chance of ignition also increases [9–11]. When ignitions coincide with extreme winds and dry fuels, rapid fire spread poses a major threat to communities. The potential for significant loss of life and property increases because fire suppression efforts have very limited success. One example of a catastrophic wind-dominated fire was the Camp Fire in 2018, which burned through the town of Paradise and is currently the deadliest (85 deaths) and most destructive (over 18,000 structures destroyed) wildfire in California history [12], with less than three hour evacuation times for many people living in Paradise.

A variety of fuels treatments are used to mitigate the severity of wildfires in fire-prone landscapes of the western United States. Commonly employed fuel-reduction treatments include clearing, thinning, surface and ladder fuel removal (also known as shaded fuel breaks), prescribed burning, planting fire-resistant vegetation, and grazing/pasturing. WUI fuel treatments of a minimum width of 400 m have been proposed to protect private property by creating safe zones for direct attack tactics [13]. Fuel treatments typically modify fire behavior but do not always stop fire growth. Fuel breaks can play an important role in controlling wildfire size and behavior if they are strategically placed, maintained, and accessible for suppression activities by firefighters [14–16]. Alternatively, structural hardening and 30–60 m of defensible space around structures can often increase fire resilience more than broad scale fuel treatments far from the WUI [1,17,18].

A recent study [1] questions the efficacy of landscape-level fuel-reduction treatments in controlling the overall size of wind-dominated fires, particularly during drought periods when fuel moisture content is very low. Most structure losses during wind-dominated wildfires are associated with spotting (burning embers lofted and transported ahead of the fire front) [12,19]. In addition to spotting, wind-dominated fires often exhibit other extreme fire behavior characteristics. High rate of spread, prolific crowning, and the presence of occasional fire whirls (vertically oriented, intensely rotating columns of gas found in or near fires) often inhibit direct fire control efforts [7]. For wind-dominated fire risks, a more effective vegetation management strategy involves increasing the fuel moisture content around the WUI [12,20], as opposed to traditional vegetation removal techniques away from the WUI. Because there is no consensus on optimal fuel break widths, more research is required to understand how fuel breaks in the WUI interact with severe downslope wind-driven fires.

Wildfire behavior modeling is one important tool in fuels management [21]. A deterministic wildfire modeling approach is one way to assess the effectiveness of fuel treatments as demonstrated by [14] and [15], because actual fire scenarios can be represented by a realization of some deterministic processes. Alternatively, a stochastic wildfire modeling approach is also used to create a more holistic picture of spatial wildfire risks using Monte Carlo simulations [22–26]. Semi-empirical fire spread models have several advantages over more sophisticated coupled fire-atmosphere models, such as significantly faster computational times and relatively simple model configurations.

The aim of this study is to explore the effectiveness of fuel breaks placed in the WUI (hereafter referred to as WUI fuel breaks) as a potential fuel treatment option for wind-dominated wildfires. We use the Camp Fire as a retrospective case study because the ignition by power line failure resulted in rapid fire spread and very short evacuation time under strong downslope winds and extremely dry fuel conditions. The main research objectives are to examine: (1) the potential downstream impacts of a WUI fuel break on fire intensity, propagation, and arrival time or evacuation time of the Camp Fire; (2) how the downstream fire behavior is affected by the width and fuel properties of the WUI fuel break; and (3) the impacts of background wind speeds on the WUI fuel break. Note that the WUI fuel break that we study is hypothetical and not an actual fuel break that exists in the study area.

2. Materials and Methods

2.1. Case Study

The Camp Fire was ignited at 06:25 Pacific Standard Time (PST) on 8 November 2018 due to an electrical transmission infrastructure failure under strong, dry downslope winds. Fuels were also very dry due to delayed autumn precipitation. The fire reached the WUI of the town of Paradise (defined here as the eastern edge of the township) within two hours (Figure 1). This rapid fire spread is speculated to have partly resulted from long-range spotting, with embers traveling as far as 7 km ahead of the main fire front [27]. Most of the burned area between Paradise and the ignition point had previously burned during the Butte Lightning Complex fire in July 2008, which was ignited by lightning strikes under hot and dry but much less windy conditions. Brewer and Clements [28] and Mass and Ovens [29] discussed the synoptic and mesoscale conditions during the Camp Fire.

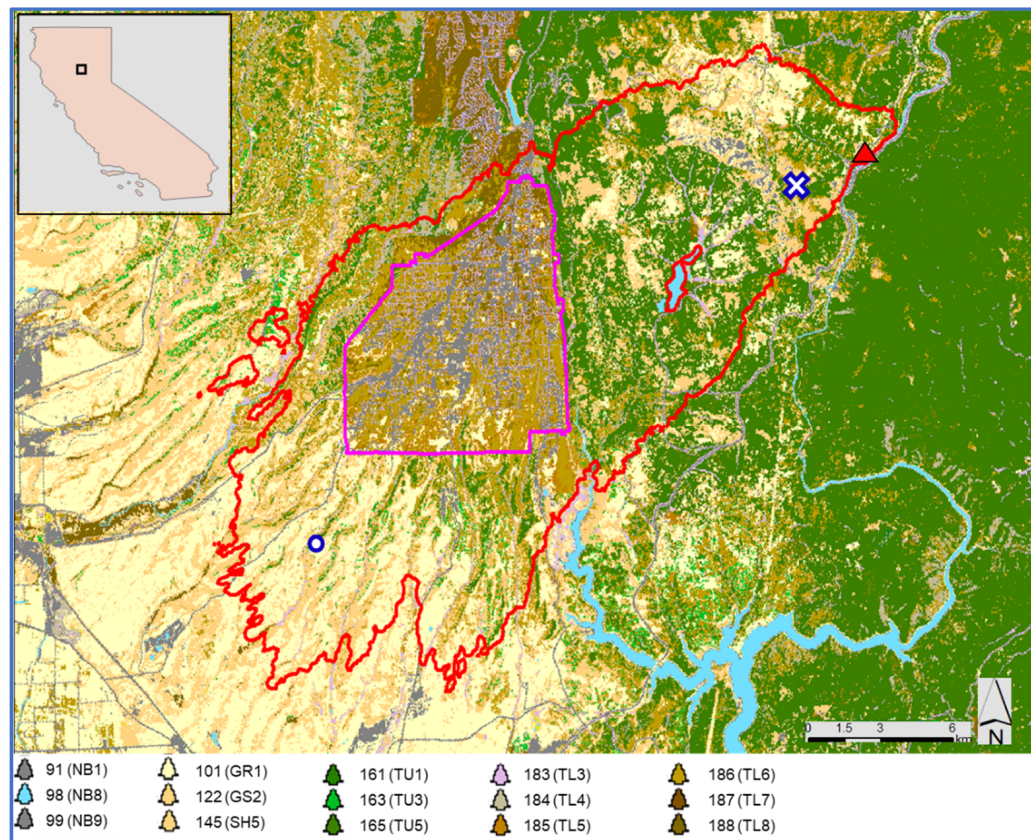


Figure 1. Map of Scott and Burgan Fire Behavior Fuel Models [30] in the 2018 Camp Fire domain. Inset shows the domain location in California, USA. Observed burn perimeter at 18:00 PST on 8 November is shown in red contour and Paradise Township boundary is shown in magenta contour. Yellow color indicates grass (GR) fuels, light orange color shrub (SH) or grass-shrub mix (GS) fuels, green color timber understory (TU) fuels, and brown color timber litter (TL) fuels in the Scott and Burgan fuel models. Bodies of water are shown in blue. The upwind (downwind) weather stream location is shown with blue cross (circle) marker. The location of the ignition is indicated with a red triangle.

2.2. Fire Growth Model

We use the Canadian operational wildland fire growth model Prometheus to test WUI fuel break sensitivity during simulations of the Camp Fire (Figure 1). Prometheus was developed to predict fire growth for near real-time operational decision support and to assess the effectiveness of various fuel management strategies [31]. It computes spatially-explicit, deterministic fire spread and behavior using topography (slope, aspect,

and elevation), fuel, and weather data as inputs. Fire perimeters are produced in time and space based on Huygen's principle of wave propagation, which is also used in the US FARSITE fire growth model [32].

Prometheus was selected for this study for the following reasons: [33] found that the FARSITE [32] and FlamMap [34] models have significant underprediction biases in modeled crown fire behavior in conifer forests in western North America. This is partly due to incompatible model linkages between Rothermel's surface [35] and crown fire [5] rate of spread models and Van Wagner's [36] criteria for crown fire initiation and propagation, which were developed independently and were not intended to work together. Rothermel's models are laboratory based, while Prometheus, which is underpinned by the Canadian Forest Fire Behavior Prediction (FBP) System [37,38], is largely based on field experiments and high-intensity wildfire observations. Prometheus also accounts for the effect of short-range spotting and breaching of non-fuel areas (lakes, rivers, roads, and fuel breaks) based on the relationship between fire intensity and flame length [39]. It also accounts for the contact angle of the head-fire to the non-fuel area [31]. Since the Camp Fire occurred in a region of mixed conifer forests, grass, shrub, and dead and down fuels, we believe that Prometheus is well suited for simulating the wildfire event and understanding the potential impact of WUI fuel breaks on wildfire behavior. Finally, fire suppression actions are not modeled as part of this study.

2.3. Weather and Fire Weather Index System Data

Hourly weather and associated Canadian Forest Fire Weather Index System component values [40,41] were used in the Prometheus fire growth simulations. For the hourly weather input, Weather Research and Forecasting (WRF) simulations were run at 1.6 km horizontal grid spacing. Model-observation comparison was conducted using surface Remote Automated Weather Station (RAWS) data in the region (Figure S1). The WRF simulation overestimated the relative humidity (RH) and wind speed for the time period between 06:30 and 18:00 PST. Overestimation trends were also seen in the WRF simulations by [28,29] that had similar horizontal grid spacing. Keeping the minor overestimations in mind, we decided to use the WRF output to create hourly weather stream data at two locations in the simulation domain (Figure 2). Meteorological inputs to Prometheus consist of an hourly time series of temperature, RH, wind speed and direction, and precipitation (hereafter weather streams). The two weather stream locations (see Figure 1) were selected to spatially represent low-level north-northwesterly flow over the northern Central Valley and strong northeasterly winds descending the western slopes of the Sierra Nevada Mountains. See [28,29] for detailed synoptic and mesoscale meteorological conditions.

We used the observed fire perimeter at 18:00 PST on 8 November 2018 to help infer biases in the wind forcing data. This is due to significant uncertainty in wind speed and direction associated with fire-atmosphere interactions [42,43] that are currently not accounted for in two-dimensional fire growth models, such as Prometheus and FARSITE. Specifically, +15 degrees was added to the hourly 10 m open wind directions to better match the simulation with the observed fire perimeter. Additionally, a gust factor, defined as the ratio between the peak wind gust of a specific duration to the mean wind speed for a period of time [44], was calculated. The 10 m hourly wind gust and horizontal wind speed (derived from u - and v -components) outputs from the ERA5 reanalysis [45] were used for the calculations. At the upwind weather input locations, we multiplied the hourly wind speeds by the gust factor. The final wind speed magnitude agrees with [29]'s estimated wind gust of $26\text{--}31 \text{ m s}^{-1}$ at the time of the ignition based on the above-surface wind speed. The final wind speed magnitude is also similar to the maximum wind speed at about 250 m above ground level in the vertical wind profiles of our WRF simulation near the ignition point at 06:00 PST (Figure S2).

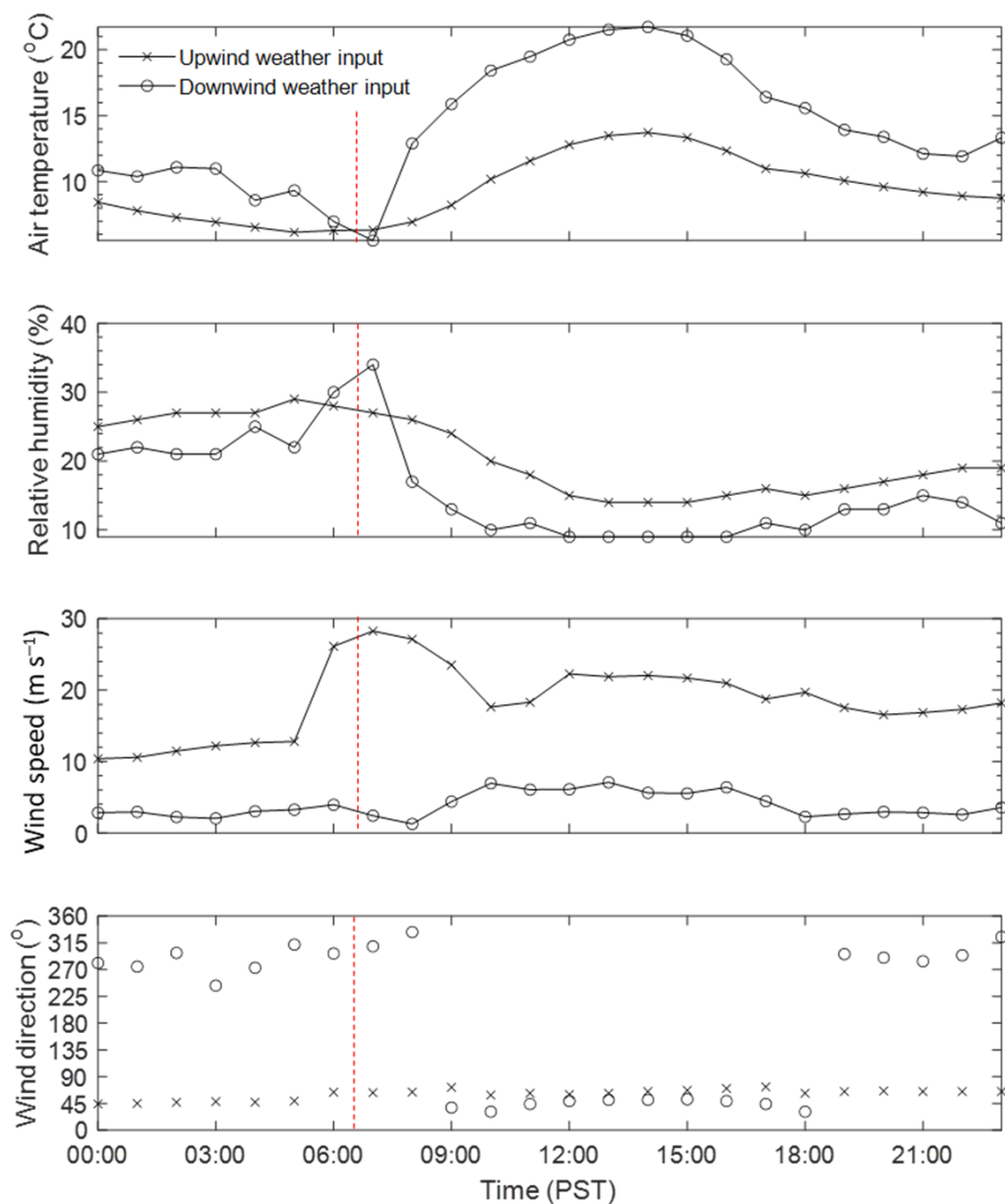


Figure 2. Input weather stream used in the Prometheus fire growth model simulations. The dashed red vertical line indicates approximate fire ignition time (06:25 PST). The locations of the upwind and downwind weather stream inputs are shown in Figure 1.

In addition to the hourly meteorological forcing, Prometheus requires Fire Weather Index System component values for the Fine Fuel Moisture Code (FFMC), Duff Moisture Code (DMC), and Drought Code (DC), to account for the effects of weather on fuel moisture contents and fire potential [40,41]. The FFMC provides a relative numeric rating of the moisture content of fine surface litter (1–2 cm depth) and is indicative of the ease of ignition and fine fuel flammability. The FFMC is characterized by a fast response to weather variations. The DMC provides a relative numerical rating of the moisture content of loosely compacted duff of moderate depth (7 cm depth) below the surface litter. The DMC has a much slower response time (15 days) than the FFMC. The DC provides a relative numerical rating of the moisture content of deep, compact organic matter (25 cm). The DC can indicate the effects of seasonal drought on forest fuels because of its long-term response time (about 53 days) to weather variations [46]. The fuel moisture code scales are arranged so that higher values represent lower moisture contents. The FFMC can range from zero to a

maximum theoretical value of 99. The DMC and DC, on the other hand, are “open ended”, meaning that they can range from zero to an increasingly higher value given an extended dry spell. The FFMC, DMC, and DC values on the day of the Camp Fire were obtained from ERA5 reanalysis. The starting FFMC, DMC, and DC values to initialize the Prometheus model were 90, 325, and 1300, respectively.

2.4. Landscape Data

In Prometheus, vegetation is represented by one of the 16 Canadian Fire Behavior Prediction System fuel types [37,38]. We converted LANDFIRE’s 40 Scott and Burgan fire behavior fuel model remap data [30,47] into the 16 standard Fire Behavior Prediction System fuel types, as shown in Figure 1 and Table 1, to better represent the domain for this case study. LANDFIRE fuel data represents structures in Paradise as non-burnable, which is not realistic. To better represent observed fire spread, we converted these fuels to M-1 with a 90% percent conifer value (Figure S3). Dominant fuel types inside the observed burn perimeter and upwind of Paradise mainly consisted of a mixture of timber understory (TU; high load conifer with shrub and grass) and timber litter (TL; dead and down woody fuel) (Figure S4). A mixture of grass and shrub fuels was more dominant downwind of Paradise. Slope, aspect, and elevation grid files for the study domain at 30 m horizontal grid spacing were also obtained from the LANDFIRE website.

Table 1. Summary of Scott and Burgan [30] fuel models with a brief description, in the LANDFIRE dataset and conversion to Canadian FBP System fuel types [37,38] used in Prometheus, and their percentage within the 2018 Camp Fire observed burn perimeter. It is noted that the 3.5 t ha^{-1} is grass fuel load default value in the FBP System (and in turn Prometheus).

Scott and Burgan (2005) Fuel Model	Brief Description	Fuel Type Assigned in Prometheus	Fuel Fractions Inside Observed Perimeter (%)
165 (TU5)	Timber-Understory. Heavy forest litter with shrub.	M-1 (90% percent conifer).	42.6
186 (TL6)	Timber Litter. Moderate fuel load.	M-1 (90% percent conifer).	14.0
188 (TL8)	Timber Litter. Moderate fuel load.	M-1 (90% percent conifer).	7.1
102 (GR2)	Low load grass.	O-1b (3.5 t ha^{-1} fuel load, 60% cured).	7.0
122 (GS2)	Grass-Shrub mixture. High spread rate.	M-1 (70% percent conifer).	6.4
91 (NB1)	Non-burnable. Urban/suburban.	Replaced by TU5.	6.1

2.5. WUI Fuel Break Design

The objective of this study is to test the effectiveness of fuel breaks around the WUI that mitigate fire speed and intensity, potentially allowing for increased evacuation time. A network of defensible fuel profile zones between 400–800 m in width has been used in the northern Sierra Nevada Mountains in California. Surface, ladder, and crown fuel loads are reduced in the zones by a combination of mechanical thinning and prescribed fire, to provide safe firefighter access and reduce fire intensity and crown fire spread [13,48,49]. There are many possible fuel break designs to be tested, with 400 m suggested as a minimum width for most WUI fuel breaks [13]. Due to the unrealistic ability to apply 400 m fuel breaks everywhere, we tested 200 m and 400 m widths. The WUI fuel breaks in our experiments were designed using Google Earth as strips along the eastern edge of the Paradise Township. These polygons were then imported into Prometheus as fuel patches (in .kml format). The WUI fuel break was placed on the eastern edge of the Paradise Township boundary because of the potential ineffectiveness of fuel breaks in remote wildland areas [16]. Because [50] showed that overlapping fuel treatment units can effectively modify fire growth and behavior, only a single strip design of a 200 m or 400 m wide WUI fuel breaks is investigated in this study.

All burnable fuels within the WUI fuel break were converted into grass fuel (O-1b fuel type), because grass fuel types in Prometheus allow for modification of grass curing and

fuel loading (the dry weight of grass in a burn unit) to represent a wide range of fuel break conditions. The grass fuel properties used for the fuel break are shown in Table S1. For simplicity, our WUI fuel break design does not account for practical considerations, such as environmental protection standards, fuel break connectivity, and fuel break aesthetics [51]. Prior to placing the WUI fuel break, 94% and 91% of the 200 m and 400 m fuel break areas were considered to be represented by variations of the FBP system fuel type M-1.

2.6. Model Evaluation and Experiments

The model performance was verified by comparing with the observed Camp Fire growth (Figure 3a). We then performed a series of sensitivity tests in which we independently varied each of the following: (i) WUI fuel break width; (ii) the degree of curing and fuel load of the grass fuel used for the WUI fuel break; and (iii) constant meteorological forcing corresponding to 06:30 PST and homogenous fuel types across the domain (tested at $\pm 25\%$ of the observed wind speed) (Tables 2 and 3).

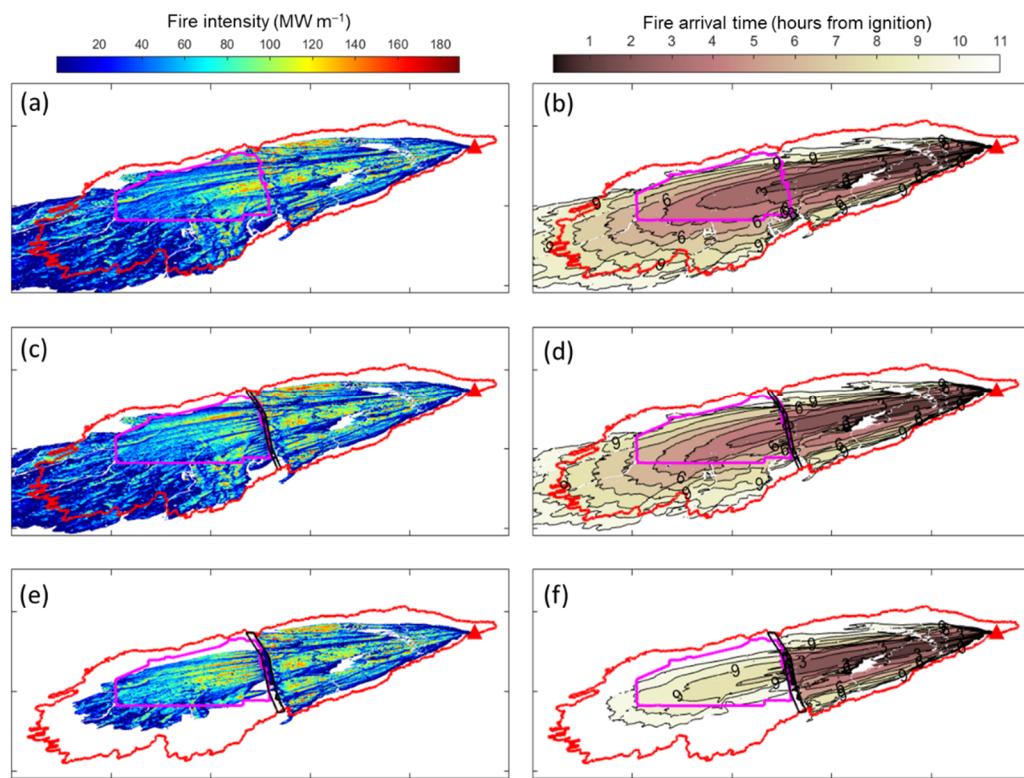


Figure 3. Simulated fire intensity (left) and fire arrival time in hours after 06:30 PST ignition (right) for the verification simulation (a,b), 200 m-wide (c,d) and 400 m-wide (e,f) WUI fuel break scenarios. The locations of the 2018 Camp Fire ignition and WUI fuel break are indicated with a red triangle and black polygon, respectively. Observed burn perimeter at 18:00 PST on 8 November is shown using a red polygon. The Paradise Township boundary is shown with a magenta polygon. In panels (a,c,e), the color bar represents fire intensity with warmer colors corresponding to higher intensities. In panels (b,d,f), the colors correspond to fire arrival times in hours since 06:30 PST, with darker colors corresponding to earlier arrival times.

Table 2. Summary of model verification and sensitivity experiments with their scenario descriptions. See Table 3 for the constant and uniform fuel specifications.

Simulation Name	Weather	Fuel	WUI Fuel Break	Scenario Description
No WUI-FB	hourly	spatially varying	No	verification run
WUI-FB200	hourly	spatially varying	YES (200 m)	added a 200-m wide WUI fuel break.
WUI-FB400	hourly	spatially varying	YES (400 m)	added a 400-m wide WUI fuel break.
WUI-FB400-DOC30	hourly	spatially varying	YES (400 m)	same as WUI-FB400 except degree of curing of grass fuel break = 30%
WUI-FB400-DOC50	hourly	spatially varying	YES (400 m)	same as WUI-FB400 except degree of curing of grass fuel break = 50%
WUI-FB400-FL1.7	hourly	spatially varying	YES (400 m)	same as WUI-FB400 except fuel load of grass fuel break halved
WUI-FB400-FL7	hourly	spatially varying	YES (400 m)	same as WUI-FB400 except fuel load of grass fuel break doubled
WUI-FB400-DOC50-FL7	hourly	spatially varying	YES (400 m)	same as WUI-FB400-DOC50 but fuel load of grass fuel break also increased by 50%
No WUI-FB U_ref	constant	uniform	No	reference run with a constant input weather stream over time
WUI-FB400 U_ref	constant	uniform	YES (400 m)	Same as above but with a 400 m WUI fuel break
WUI-FB400 U_lower	constant	uniform	YES (400 m)	with a 400 m WUI fuel break and 25% lower wind speed than reference run
WUI-FB400 U_higher	constant	uniform	YES (400 m)	with a 400 m WUI fuel break and 25% higher wind speed than reference run

Table 3. Constant upwind weather stream input used for the idealized experiments in Sections 2.5 and 2.6.

Temp (°C)	RH (%)	WS (m s ⁻¹)	WD (°)	Fuel Type
6.3	28	20, 26, 32	64	M-1 (90pc)

3. Results

3.1. Model Calibration

Figure 3a,b show the simulation output of fire arrival time and fire intensity 11.5 h after ignition. The simulated fire arrival time to the eastern edge of the Paradise boundary was between two and three hours, whereas the actual Camp Fire may have travelled and/or spotted there as quickly as 1.5 h after ignition [52]. An estimation of fire arrival time at Paradise can be made using the equation in [53]: the forward rate of fire spread measurement R (km h⁻¹) = d/t , where d represents the maximum distance (km) from the end point of one fire isochrone to the end point of the preceding isochrone over a given time period t (h), can be rewritten as $t = d/R$. Using the distance of 11 km between Paradise and the ignition point and the observed $R = 4\text{--}4.8$ as shown in [53], we found a fire arrival time of 2 h 20 min–2 h 30 min to Paradise.

Model-derived fire intensity is one of the critical parameters for understanding the potential for high intensity forest fire behavior. Fire intensity is also used for fuel treatment prescriptions [24]. The simulated fire intensity (Figure 3a) shows areas over 100 MW m⁻¹ associated with an active/continuous crown fire (Crown Fraction Burned > 90%; not shown) upstream of Paradise compared to the downstream area. Lower fire intensity occurs in locations where the grass fuel type is dominant. Observations show the simulated fire intensity reasonably, as the fire intensity of wind-dominated crown fires has been observed to exceed 100 MW m⁻¹ for significant periods of time. For example, a head fire intensity of 90 MW m⁻¹ was observed in a northern jack pine-black spruce forest during a crown fire experiment in Canada. Fuel consumptions in that experiment ranged from 2.8 to 5.5 kg m⁻² [54]. Simulated total fuel consumptions in this study were on average 4.5 kg m⁻² for the forest fuel types.

Computed mean rate of spread and fire intensity for forest and grass fuel types for the verification run are shown in Figure 4. The mean modeled rate of spread was close to 60 m min^{-1} for the forest fuel types for the first three hours after ignition, when the input wind speed was also the highest. Maranghides et al. [26] estimated the fire spread rate during the Camp Fire to be 66 m min^{-1} for the first hour and 60 m min^{-1} in the grass areas downwind of Paradise. Therefore, overall modeled mean rate of spread of $20\text{--}30 \text{ m min}^{-1}$ for the simulated grass fuel may be underestimated, given that model parameters associated with complete (100%) curing were not used because the model substantially overestimated observed fire growth rate. However, assigning the degree of curing value of 100% for the grass fuels in the entire domain in our simulation resulted in a significant overestimation of the fire growth downwind of Paradise. A much larger fraction of the hourly burned area was more dominated by the forest fuel types compared to the grass fuel types in our simulations. Therefore, the impact of the underestimated rate of spread on the simulated fire arrival time at Paradise was relatively small. After calibration, the overall shape of the fire perimeter is well represented in the model and serves as a good reference for fuel modification experiments.

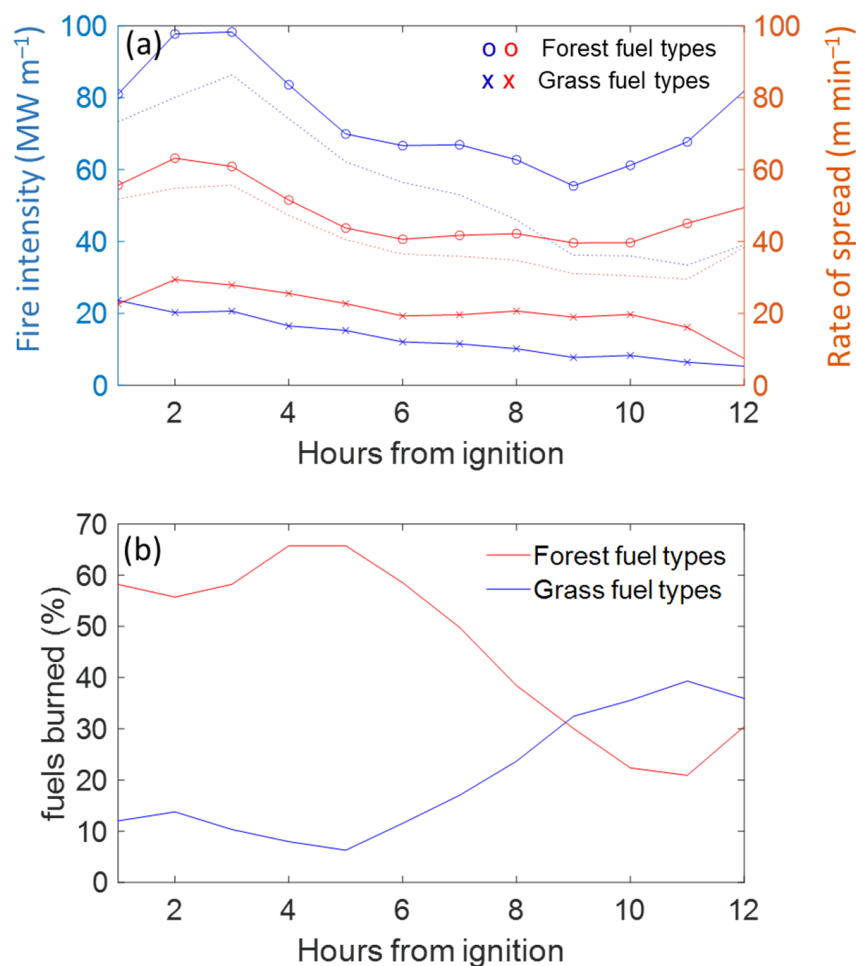


Figure 4. Simulated hourly (a) fire intensity (blue) and rate of spread (red) of the 2018 Camp Fire, and (b) proportion of area burned per hour for forest compared to grass fuel types. Dashed lines in (a) indicate hourly averages for all fuel types burned for the hour.

3.2. Impact of WUI Fuel Breaks on Downstream Fire Behavior

Figure 5 shows the results of fire intensity for the verification run (no WUI fuel break) and the 200 m and 400 m WUI fuel break runs. Both fuel break simulations dispersed the fire front downstream of the fuel break. Fire intensity increased downstream of the

400 m fuel break, as compared to the no-fuel break scenario. This is likely resulting from interactions between the fire spread rate and timing of the meteorological forcing. That is, relative humidity dropped from the morning into the afternoon concomitantly with the fire's leading edge moving downstream of the fuel break. Flank fire (lateral fire spread) was also noticeably suppressed downstream of the 400 m fuel break, because a delay in fire spread across the WUI fuel break means less time for the forward and lateral fire spread.

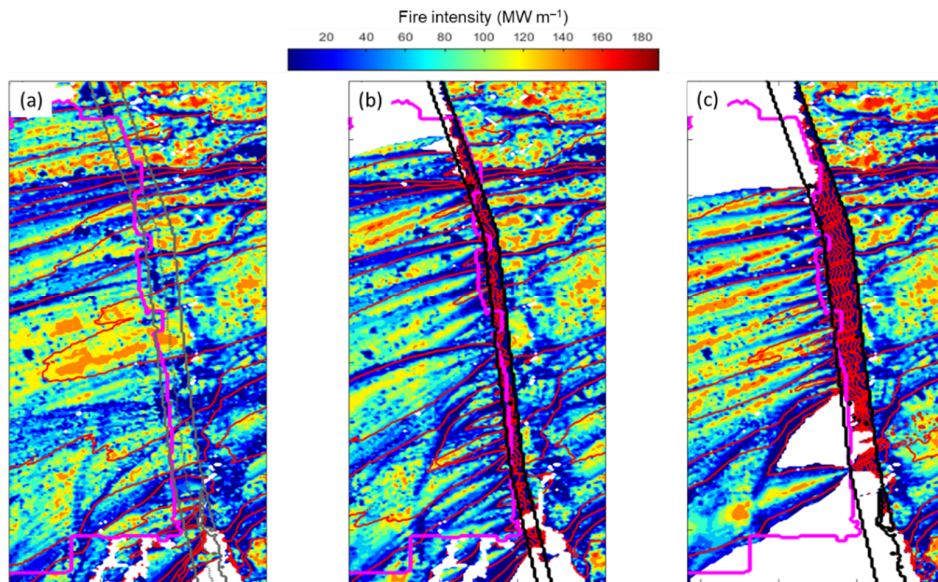


Figure 5. Simulated fire intensity of the 2018 Camp Fire for the: (a) no WUI-FB; (b) WUI-FB200; and (c) WUI-FB400 scenarios. Red contours indicate fire propagations and thick magenta lines indicate the Paradise Township boundary. The locations of the WUI fuel break are indicated by a black polygon. The WUI fuel break location shown in (a) is only for reference.

One way to measure the effectiveness of the WUI fuel break in the context of wind-dominated wildfires ignited near the WUI is the time gained for community evacuation during a fast-approaching wildfire. Figure 6 shows the area burned in Paradise (inside the magenta isoline in Figure 1) over the simulation time. While the 200 m fuel break delayed the fire arrival by an hour as compared to the verification run with no fuel break, the 400 m fuel break resulted in a five-hour delay. These one- and five-hour delays in fire arrival time at Paradise represent the potential evacuation time that could have been afforded to Paradise by WUI fuel breaks. It should also be noted that at the end of the simulations, the 200 (400) m fuel break scenario resulted in 0.8% (15.5%) of the area saved in Paradise, as compared to the no fuel break scenario that showed 99.3% of the burned area in Paradise.

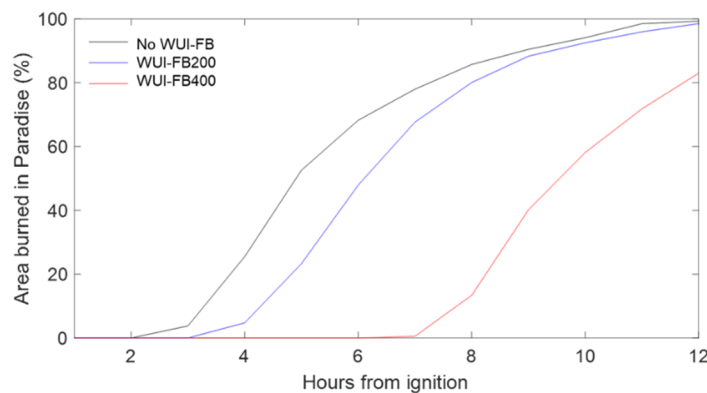


Figure 6. Percent of area burned in Paradise (inside the magenta polygon in Figure 1) vs. time after ignition in hours for the 2018 Camp Fire verification run, 200 m and 400 m WUI fuel break runs.

3.3. Impact of the Grass Fuel Conditions over the WUI Fuel Break on Downstream Fire Propagation

Changing the fuel load of the grass fuel over the WUI fuel break from 3.5 t ha^{-1} (WUI-FB400) to 1.7 t ha^{-1} (WUI-FB400-FL1.7), or 7 t ha^{-1} (WUI-FB400-FL7) had little impacts on the area burned in Paradise over the simulation time (Figure 7). This is because in the FBP system the fuel load does not affect the rate of fire spread in grass fuel type O-1, but it does affect fire intensity. Conversely, the dryness of the grass, as represented by the degree of curing in this study, played a major role in the area burned. When a 50% value was used for the degree of curing, the area burned approached the verification model scenario with no fuel break present. Fuel load played little role in fire intensity of the grass fuel in the fuel break as the range of the fuel load values resulted in similar fire intensity (Figure 7b). Overholt et al. [55] similarly found that fuel moisture content of the grass fuel played the most significant role in the fire spread rate, whereas the fuel load did not play a major role in the fire spread rate.

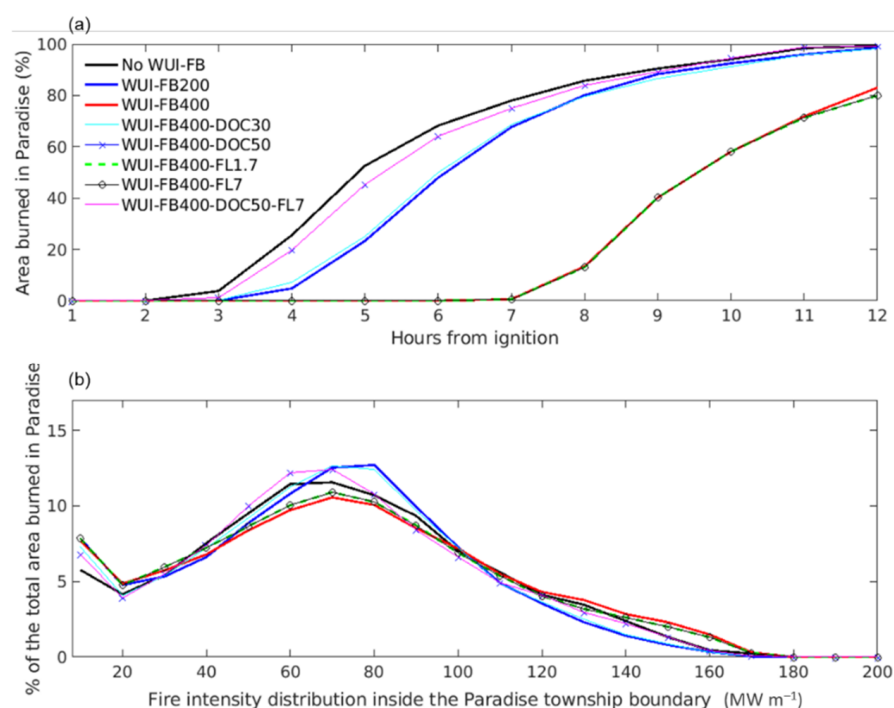


Figure 7. Plots showing (a) time vs. total area burned in Paradise (inside the magenta polygon in Figure 1) and (b) fire intensity distribution for the 2018 Camp Fire simulations. Refer to Table 2 for the experimental settings for each simulation name.

For the degree of curing of 10% and fuel load of 3.5 t ha^{-1} , the increased fuel break width from the 200 m to 400 m resulted in decreased fire intensity over the $50\text{--}100 \text{ MW m}^{-1}$ and increased fire intensity over the $110\text{--}170 \text{ MW m}^{-1}$ range. This result possibly occurred from the interaction between the WUI fuel break and daytime progression of weather. The fire intensity distributions in Figure 7 are reflected in the fire intensity maps in Figure 3 that show locally higher fire intensity over Paradise in the 400 m WUI fuel break scenario (Figure 3e), as compared to the 200 m one (Figure 3c). It is possible that, as a result of delayed fire arrival time to Paradise, higher air temperatures and lower RH midday caused more severe burning conditions despite lower input wind speeds.

3.4. Role of Wind Speeds in the Effectiveness of WUI Fuel Breaks

In this section, three simulations were run using three different constant wind speeds ($20, 26,$ and 32 m s^{-1}) over a uniform fuel landscapes (M-1 with a 90% percent conifer value). Weather inputs were kept the same over the entire simulation, as shown in Table 3. The objective of this analysis was to determine the impacts of wind speeds on the effectiveness of the WUI fuel breaks. Figure 8 shows the simulated burn perimeters for 25% lower and 25% higher wind speeds than the reference simulation (26 m s^{-1}). For increased (decreased) wind speeds, the fire perimeters became narrower (wider) as compared to the fire perimeter with the reference wind speed both upstream and downstream of the fuel break. Thus, the burned area in Paradise was controlled not only by the fuel break, but also wind speed timing relative to ignition timing, such that lower wind speeds resulted in broader, shorter fire perimeters (Figure 8).

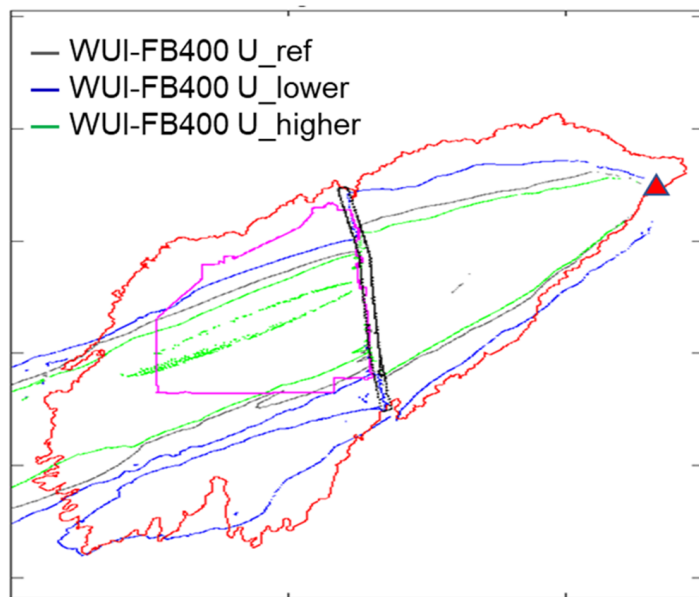


Figure 8. Contour line plot of fire arrival time at time = 11.5 h into the simulation for the reference constant wind speed (WUI-FB400 U_ref), and 25% lower (WUI-FB400 U_lower) and 25% higher (WUI-FB400 U_higher) than the reference wind speeds. The locations of the ignition and WUI fuel break are indicated with a red triangle and black polygon, respectively. The red contour line indicates the observed burn perimeter at 18:00 PST on 8 November. The Paradise Township boundary is shown by a magenta polygon.

Figure 9a shows the percent area burned in Paradise over the simulation time. The simulation with the highest wind speed (WUI-FB400_higher) resulted in the lowest percent area burned in Paradise at the end of the simulations due to narrower fire perimeters. These results can depend on the behavior of the fire front. The highest wind speed did not necessarily result in the earliest fire arrival at Paradise because the fire propagation speed over the WUI fuel break appeared to depend on the upstream fire propagation and its approaching direction to the WUI fuel break. Figure 9b shows the fire intensity distribution of burned area in Paradise for three different wind speeds. There is evidence that wind speed played a role in modifying the fire intensity as expected. For example, the lower wind speed simulation (blue line) resulted in less areas of relatively high fire intensity around 160 MW m^{-1} and more areas with lower fire intensity around 100 MW m^{-1} as compared to the higher wind speed simulation (red line). However, the dominant fire intensity remained at 160 MW m^{-1} regardless of wind speeds. It is also shown that a 400 m wide fuel break has a minor effect in reducing fire intensity downstream from 180 to 160 MW m^{-1} , which still remains well above the suppression threshold of 3 MW m^{-1} considered effective for airtankers controlling a fireline [56].

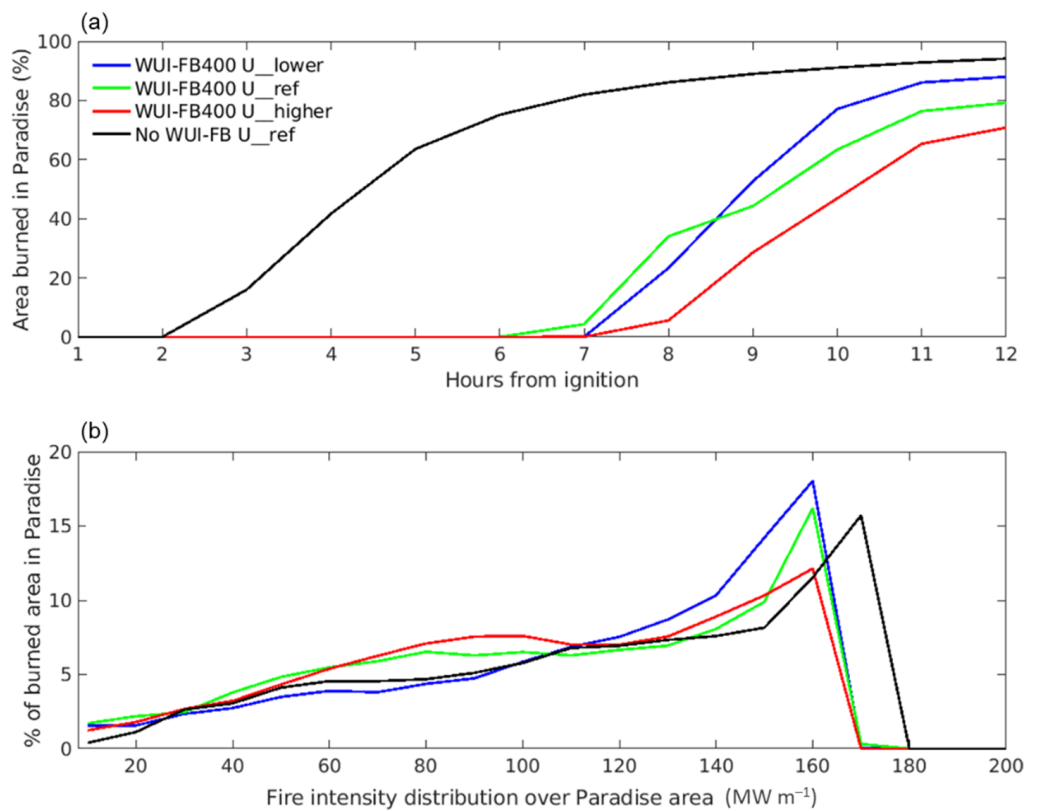


Figure 9. (a) Time vs. area burned in Paradise and (b) fire intensity distribution vs. percent of the total area burned in Paradise at the end of the simulations with three different constant wind speed inputs. See Tables 2 and 3 for the experimental settings of each simulation name.

4. Discussion

This study investigated the effectiveness of WUI fuel breaks on downslope wind-dominated fire behavior, including fire intensity and spread rate. Both directly impact WUI community evacuation time and wildfire damage potential. We found that increasing the width of a WUI fuel break from 200 m to 400 m more than doubled the evacuation time. In addition, the fuel break changed fire behavior by breaking up the advancing fire front into multiple fire fronts on the downstream edge of the fuel break. However, the overall fire intensity downstream of the fuel break remained well above the suppression threshold intensity. Furthermore, the width and degree of curing in grass fuel comprising the WUI fuel break had noticeable impacts on controlling fire arrival and evacuation times downstream of the WUI fuel break. Finally, we showed that the burned area downstream of the WUI fuel break may be affected by both the presence of the fuel break and magnitude of the extreme wind speeds. The latter controlled the lateral extent of fire spread upstream of the fuel break.

While our model experiments provide evidence for the potential utility of WUI fuel breaks in mitigating wildfire hazards, there are several sources of uncertainty rooted in model assumptions. For example, Prometheus does not represent long-range spotting. We acknowledge that not including the influence of long-range spotting in our simulation runs is a limitation of this work, as 200–400 m spotting distances are common [57]. From an observational perspective, it is unclear whether long-range spotting contributed to the increased rate of spread or if the head fire overran the spot fire ignitions during the Camp Fire. Storey et al. [58] found that the contribution of spot fires to the overall rate of spread may depend on topography. In their study, spotting accelerated the spread of the fire front in complex terrains. The Camp Fire region is topographically complex and thus, the spot fires may have contributed to uncertainty in model predictions. Operational two-dimensional fire growth models, including Prometheus and FARSITE, also do not currently

account for atmospheric stability, which is known to be a major contributor to long-range spotting and nonlinear fire spread and intensity [59]. Another source of uncertainty is fuel moisture content in the WUI fuel breaks, which we were unable to directly modify. The effect of the FFMC on fire spread was also examined by using a weather patch function in Prometheus to produce rainfall over the WUI fuel break. The precipitation lowered the FFMC value and resulted in substantial reductions in the burned area (Figure S5). The combined effects of the FFMC and the degree of curing on the WUI fuel break effectiveness warrant further investigation using a set of similar experiments.

The grass fuel type in the WUI fuel breaks tested in this study can be viewed as the most optimistic scenario, as it may be prohibitively expensive to remove trees in the WUI fuel breaks. In our study, we explored a scenario in which all existing trees were converted to grass without leaving any additional fuels on the ground. In reality, more live and dead fuels may be distributed in patches on the ground after a fuel treatment. Partial tree removal is expected to increase evacuation times relative to no WUI fuel break, but not by as much as a fuel break with no trees.

Even though only grass type WUI fuel breaks were explored in this study, varying the degree of curing and fuel load scenarios may represent alternative designs of WUI fuel breaks with similar fire behavior characteristics of the grass fuel type. Agricultural lands, open space parks and preserves, golf courses, and other recreational green zones (i.e., greenbelts) have been proposed or already implemented to create wildfire resilient communities in some parts of California [60]. Similar assessments of proposed WUI fuel breaks can be conducted to estimate relative evacuation time gains using operational or more sophisticated fire spread models for different fuel break designs and historical weather scenarios. In practice, the design and implementation of greenbelts or WUI fuel breaks requires collaboration and coordination efforts among cities and counties, landowners, and local agencies, such as fire departments and regional park services [13,60]. Furthermore, an often-overlooked requirement for the construction of WUI fuel breaks is that when firefighters deploy, there must be an adequate number of firefighter safety zones established along the fuel break [61].

California wildfires forced the evacuation order of over one million residents in California during 2017–2019 [62]. Increasing population and WUI expansion increase the likelihood of human-caused ignitions [12]. Thus, community evacuations may become more important than in the past to minimize the impacts of wind-dominated fires. Community evacuations during extreme wind-dominated wildfires may pose considerable challenges and stresses on emergency management agencies, as seen during the Camp Fire. Our results suggest that WUI fuel breaks, if constructed sufficiently wide and green (i.e., degree of curing), are beneficial for delaying fire front arrival and gaining evacuation times by several hours.

Currently, California plans to spend \$1.5 billion on vegetation management in 2021 [63]. Greenbelts constructed on the fringe of urban areas are one promising way to spend these funds and may also be able to reduce overall firefighting costs. They also have the potential to create fire resilient communities, while promoting positive social, economic, and environmental impacts. The primary goal of this work was to quantitatively understand the effectiveness of hypothetical WUI fuel breaks and their interactions with wind-dominated high intensity crown fires under extreme fire weather conditions. Our study contributed to these goals by quantitatively understanding the effectiveness of hypothetical WUI fuel breaks and their interactions with wind-dominated high intensity crown fires under an extreme fire weather condition. To make these experiments more realistic, a combination of topography, location, land use, environmental constraints, ecological impacts, and implementation costs should be incorporated into fire growth simulations with fuel breaks.

5. Conclusions

The model simulations presented in this study indicate that WUI fuel breaks would have afforded more evacuation time for the town of Paradise. The results of reduced final burned area and locally reduced fire intensity downstream of the WUI fuel break in our simulations also suggest that total area burned and home destruction would have possibly been lower. It is hypothesized that structural hardening and creating a proper defensible space around homes can minimize the impact of long-range spotting crossing the WUI fuel breaks and the risk of urban conflagrations. To best prepare communities for unexpected circumstances, a myriad of other measures could be deployed, including evacuation planning and community education.

On a concluding note, this study does not include all facets of wildfire dynamics. Future research could also utilize several different wildfire growth models to examine the relative effectiveness of existing or planned WUI fuel breaks and greenbelts. The increasing amount of wildfire-related remote sensing data could be used to examine how wildfires have behaved in already existing greenbelts and WUI fuel breaks.

Supplementary Materials: The following supporting information can be downloaded at: <https://www.mdpi.com/article/10.3390/fire5020037/s1>. Figure S1: WRF model verification; Figure S2: Vertical wind profiles of the WRF simulation; Figure S3: Impact of non-burnable housing structures on fire spread simulations; Figure S4: Dominant fuel types inside the observed burn perimeter; Figure S5: Impact of FFMC on fire spread; Table S1: Grass fuel properties used for the fuel break.

Author Contributions: Conceptualization, D.S., C.J., A.T.T., K.V., A.J.P., L.M.V.C., C.T., J.G. and K.D.; methodology, D.S., C.J., A.T.T., K.V., A.J.P., L.M.V.C., C.T., J.G. and K.D.; validation, D.S.; formal analysis, D.S.; data curation, D.S.; writing—original draft preparation, D.S.; writing—review and editing, D.S., C.J., A.T.T., K.V., A.J.P., L.M.V.C., C.T., J.G. and K.D.; visualization, D.S.; supervision, C.J.; project administration, D.S. and C.J.; funding acquisition, C.J., A.T.T., A.J.P. and L.M.V.C. All authors have read and agreed to the published version of the manuscript.

Funding: This research was funded by the University of California Office of the President Laboratory Fees Program (Grant ID: LFR-20-652467). K. Varga was supported by the NASA Future Investigators in NASA Earth and Space Science and Technology program (Award no. 80NSSC21K1630).

Data Availability Statement: Copernicus Climate Change Service: ERA5: Fire danger indices historical data from the Copernicus Emergency Management Service. DOI: 10.24381/cds.0e89c522. LANDFIRE: us_200_40 Scott and Burgan Fire Behavior Fuel Models. U.S. Department of Interior, Geological Survey, and U.S. Department of Agriculture. [Online]. Available: <http://landfire.cr.usgs.gov/viewer/>, accessed on 24 October 2020. Observed perimeter data: Perimeters DD83. Available: http://rmgsc.cr.usgs.gov/outgoing/Geomac/historic_fire_data, accessed on 21 September 2020.

Acknowledgments: The authors would like to acknowledge the high-performance computing support from Cheyenne (<https://doi.org/10.5065/D6RX99HX>; accessed on 15 November 2020) provided by the National Center for Atmospheric Research (NCAR) Computational and Information Systems Laboratory, sponsored by the National Science Foundation. The authors thank the European Centre for Medium-Range Weather Forecasts for making the ERA5 Reanalysis available. ERA5 reanalysis was obtained from the Research Data Archive at NCAR Computational and Information Systems Laboratory (<https://doi.org/10.5065/BH6N-5N20N>; accessed on 28 November 2020). We also thank Neal McLoughlin at Agriculture and Forestry Wildfire Management Branch in Edmonton, Canada for his time on Prometheus technical help and discussion.

Conflicts of Interest: The authors declare no conflict of interest.

References

1. Keeley, J.E.; Syphard, A.D. Twenty-first century California, USA, wildfires: Fuel-dominated vs. wind-dominated fires. *Fire Ecol.* **2019**, *15*, 24. [[CrossRef](#)]
2. Byram, G.M. Forest fue behavior. In *Forest Fire: Control and Use*; Davis, K.P., Ed.; McGraw-Hill: New York, NY, USA, 1959; pp. 90–123.
3. Kiefer, M.T.; Parker, M.D.; Charney, J.J. Regimes of Dry Convection above Wildfires: Idealized Numerical Simulations and Dimensional Analysis. *J. Atmos. Sci.* **2009**, *66*, 806–836. [[CrossRef](#)]

4. Morvan, D. Wind Effects, Unsteady Behaviors, and Regimes of Propagation of Surface Fires in Open Field. *Combust. Sci. Technol.* **2014**, *186*, 869–888. [[CrossRef](#)]
5. Rothermel, R.C. *Predicting Behavior and Size of Crown Fires in the Northern Rocky Mountains*; Research Paper INT438; United States Department of Agriculture, Forest Service, Intermountain Research Station: Ogden, UT, USA, 1991; p. 46. [[CrossRef](#)]
6. Keeley, J.E.; Syphard, A. Historical patterns of wildfire ignition sources in California ecosystems. *Int. J. Wildland Fire* **2018**, *27*, 781. [[CrossRef](#)]
7. Werth, P.A.; Potter, B.E.; Alexander, M.E.; Clements, C.B.; Cruz, M.G.; Finney, M.A.; Forthofer, J.M.; Goodrick, S.L.; Hoffman, C.; Jolly, W.M.; et al. *Synthesis of Knowledge of Extreme Fire Behavior: Volume 2 for Fire Behavior Specialists, Researchers, and Meteorologists*; General Technical Reports PNW-GTR-891; Department of Agriculture, Forest Service, Pacific Northwest Research Station: Portland, OR, USA, 2016; p. 258.
8. Countryman, C.M. Can Southern California Wildland Conflagrations be Stopped? In *General Technical Report, PSW-7*; USDA Forest Service, Pacific Southwest Forest and Range Experiment Station: Berkeley, CA, USA, 1974; pp. 1–11.
9. Abatzoglou, J.T.; Balch, J.K.; Bradley, B.A.; Kolden, C. Human-related ignitions concurrent with high winds promote large wildfires across the USA. *Int. J. Wildland Fire* **2018**, *27*, 377. [[CrossRef](#)]
10. Balch, J.K.; Bradley, B.A.; Abatzoglou, J.T.; Nagy, R.C.; Fusco, E.J.; Mahood, A.L. Human-started wildfires expand the fire niche across the United States. *Proc. Natl. Acad. Sci. USA* **2017**, *114*, 2946–2951. [[CrossRef](#)]
11. Radeloff, V.C.; Helmers, D.P.; Kramer, H.A.; Mockrin, M.H.; Alexandre, P.M.; Bar-Massada, A.; Butsic, V.; Hawbaker, T.J.; Martinuzzi, S.; Syphard, A.D.; et al. Rapid growth of the US wildland-urban interface raises wildfire risk. *Proc. Natl. Acad. Sci. USA* **2018**, *115*, 3314–3319. [[CrossRef](#)]
12. Syphard, A.; Keeley, J. Factors Associated with Structure Loss in the 2013–2018 California Wildfires. *Fire* **2019**, *2*, 49. [[CrossRef](#)]
13. Safford, H.D.; Schmidt, D.A.; Carlson, C.H. Effects of fuel treatments on fire severity in an area of wildland–urban interface, Angora Fire, Lake Tahoe Basin, California. *For. Ecol. Manag.* **2009**, *258*, 773–787. [[CrossRef](#)]
14. Agee, J.K.; Bahro, B.; Finney, M.A.; Omi, P.N.; Sapsis, D.B.; Skinner, C.N.; van Wagtendonk, J.W.; Weatherspoon, C.P. The use of shaded fuelbreaks in landscape fire management. *For. Ecol. Manag.* **2000**, *127*, 55–66. [[CrossRef](#)]
15. Oliveira, T.M.; Barros, A.M.G.; Ager, A.A.; Fernandes, P.M. Assessing the effect of a fuel break network to reduce burnt area and wildfire risk transmission. *Int. J. Wildland Fire* **2016**, *25*, 619–632. [[CrossRef](#)]
16. Syphard, A.D.; Keeley, J.E.; Brennan, T.J. Factors affecting fuel break effectiveness in the control of large fires on the Los Padres National Forest, California. *Int. J. Wildland Fire* **2011**, *20*, 764–775. [[CrossRef](#)]
17. Gibbons, P.; Van Bommel, L.; Gill, A.M.; Cary, G.J.; Driscoll, D.A.; Bradstock, R.A.; Knight, E.; Moritz, M.A.; Stephens, S.L.; Lindenmayer, D.B. Land Management Practices Associated with House Loss in Wildfires. *PLoS ONE* **2012**, *7*, e29212. [[CrossRef](#)] [[PubMed](#)]
18. Syphard, A.D.; Brennan, T.J.; Keeley, J.E. The role of defensible space for residential structure protection during wildfires. *Int. J. Wildland Fire* **2014**, *23*, 1165–1175. [[CrossRef](#)]
19. Cohen, J.D.; Stratton, R.D. *Home Destruction Examination: Grass Valley Fire, Lake Arrowhead, California*; Tech. Paper R5-TP-026b; U.S. Department of Agriculture, Forest Service, Pacific Southwest Region (Region 5): Vallejo, CA, USA, 2008; p. 26. Available online: <https://www.fs.usda.gov/treesearch/pubs/31544> (accessed on 24 November 2021).
20. Gibbons, P.; Gill, A.M.; Shore, N.; Moritz, M.A.; Dovers, S.; Cary, G.J. Options for reducing house-losses during wildfires without clearing trees and shrubs. *Landsc. Urban Plan.* **2018**, *174*, 10–17. [[CrossRef](#)]
21. Varner, J.; Keyes, C. Fuels treatments and fire models: Errors and corrections. *Fire Manag. Today* **2009**, *69*, 47–50.
22. Ager, A.A.; Finney, M.A.; Kerns, B.K.; Maffei, H. Modeling wildfire risk to northern spotted owl (*Strix occidentalis caurina*) habitat in Central Oregon, USA. *For. Ecol. Manag.* **2007**, *246*, 45–56. [[CrossRef](#)]
23. Carmel, Y.; Paz, S.; Jahashan, F.; Shoshany, M. Assessing fire risk using Monte Carlo simulations of fire spread. *For. Ecol. Manag.* **2009**, *257*, 370–377. [[CrossRef](#)]
24. Cruz, M.G.; Alexander, M.E. Modelling the rate of fire spread and uncertainty associated with the onset and propagation of crown fires in conifer forest stands. *Int. J. Wildland Fire* **2017**, *26*, 413–426. [[CrossRef](#)]
25. Finney, M.A.; Grenfell, I.C.; McHugh, C.W.; Seli, R.C.; Trethewey, D.; Stratton, R.D.; Brittain, S. A Method for Ensemble Wildland Fire Simulation. *Environ. Model. Assess.* **2011**, *16*, 153–167. [[CrossRef](#)]
26. Ramirez, J.; Monedero, S.; Silva, C.; Cardil, A. Stochastic decision trigger modelling to assess the probability of wildland fire impact. *Sci. Total Environ.* **2019**, *694*, 133505. [[CrossRef](#)] [[PubMed](#)]
27. Maranghides, A.; Link, E.; Mell, W.; Hawks, S.; Wilson, M.; Brewer, W.; Brown, C.; Vihianeck, B.; Walton, W.D. *A Case Study of the Camp Fire—Fire Progression Timeline*; Technical Note (NIST TN), National Institute of Standards and Technology: Gaithersburg, MD, USA, 2021. [[CrossRef](#)]
28. Brewer, M.J.; Clements, C.B. The 2018 Camp Fire: Meteorological Analysis Using In Situ Observations and Numerical Simulations. *Atmosphere* **2020**, *11*, 47. [[CrossRef](#)]
29. Mass, C.F.; Ovens, D. The Synoptic and Mesoscale Evolution Accompanying the 2018 Camp Fire of Northern California. *Bull. Am. Meteorol. Soc.* **2020**, *102*, E168–E192. [[CrossRef](#)]
30. Scott, J.H.; Burgan, R.E. *Standard Fire Behavior Fuel Models: A Comprehensive Set for Use with Rothermel's Surface Fire Spread Model*; US Department of Agriculture, Forest Service, Rocky Mountain Research Station: Fort Collins, CO, USA, 2005; p. 153. [[CrossRef](#)]

31. Tymstra, C.; Bryce, R.W.; Wotton, B.M.; Taylor, S.W.; Armitage, O.B. *Development and Structure of Prometheus: The Canadian Wildland Fire Growth Simulation Model*; Information Report NOR-X-417; Natural Resources Canada, Canadian Forest Service, Northern Forestry Centre: Edmonton, AB, Canada, 2010.
32. Finney, M. *FARSITE Fire Area Simulator Model Development and Evaluation*; Res. Pap. RMRS-RP-4, Revised 2004; U.S. Department of Agriculture, Forest Service, Rocky Mountain Research Station: Ogden, UT, USA, 1998; p. 47.
33. Cruz, M.G.; Alexander, M.E. Assessing crown fire potential in coniferous forests of western North America: A critique of current approaches and recent simulation studies. *Int. J. Wildland Fire* **2010**, *19*, 377–398. [CrossRef]
34. Finney, M. An Overview of FlamMap Fire Modeling Capabilities. In Proceedings of the Fuels Management—How to Measure Success: Conference Proceedings, Portland, OR, USA, 28–30 March 2006; Proceedings RMRS-P-41. Andrews Patricia, L., Butler Bret, W., Eds.; U.S. Department of Agriculture, Forest Service, Rocky Mountain Research Station: Fort Collins, CO, USA, 2006; pp. 213–220.
35. Rothermel, R.C. A Mathematical Model for Predicting Fire Spread in Wildland Fuels. In *Research Paper*; INT-115; USDA Forest Service, Intermountain Forest and Range Experiment Station: Ogden, UT, USA, 1972; pp. 1–40.
36. Van Wagner, C.E. Conditions for the start and spread of crown fire. *Can. J. For. Res.* **1977**, *7*, 23–34. [CrossRef]
37. Forestry Canada Fire Danger Group. *Development of the Canadian Forest Fire Behavior Prediction System*; Information Report ST-X-3; Canadian Forest Service Publications: Sault Ste. Marie, ON, Canada, 1992; Volume 3, p. 66. Available online: https://cfs.nrcan.gc.ca/publications?id=10068%0Ahttps://www.frames.gov/documents/catalog/forestry_canada_fire_danger_group_1992.pdf (accessed on 24 November 2021).
38. Wotton, B.M.; Alexander, M.E.; Taylor, S.W. *Updates and Revisions to the 1992 Canadian Forest Fire Behavior Prediction System*; Information Report GLC-C-10E; Natural Resources Canada Forest Service, Great Lakes Forestry Centre: Sault Ste. Marie, ON, Canada, 2009; p. 45.
39. Byram, G.M. Combustion of forest fuels. In *Forest Fire: Control and Use*; Davis, K.P., Ed.; McGraw-Hill: New York, NY, USA, 1959; pp. 61–89.
40. Van Wagner, C.E. *Development and Structure of the Canadian Forest Fire Weather Index System*; Forestry Technical Report 35; Government of Canada, Canadian Forestry Service: Ottawa, ON, Canada, 1987. Available online: <https://d1ied5g1xfgpx8.cloudfront.net/pdfs/19927.pdf> (accessed on 24 November 2021).
41. Lawson, B.D.; Armitage, O.B. *Weather Guide for the Canadian Forest Fire Danger Rating System*; Natural Resources Canada, Canadian Forest Service, Northern Forestry Centre: Edmonton, AB, Canada, 2008; p. 73.
42. Clements, C.B.; Kochanski, A.K.; Seto, D.; Davis, B.; Camacho, C.; Lareau, N.P.; Conteza, J.; Restaino, J.; Heilman, W.E.; Krueger, S.K.; et al. The FireFlux II experiment: A model-guided field experiment to improve understanding of fire–atmosphere interactions and fire spread. *Int. J. Wildland Fire* **2019**, *28*, 308. [CrossRef]
43. Srock, A.F.; Charney, J.J.; Potter, B.E.; Goodrick, S.L. The Hot-Dry-Windy Index: A New Fire Weather Index. *Atmosphere* **2018**, *9*, 279. [CrossRef]
44. Paulsen, B.M.; Schroeder, J.L. An Examination of Tropical and Extratropical Gust Factors and the Associated Wind Speed Histograms. *J. Appl. Meteorol.* **2005**, *44*, 270–280. [CrossRef]
45. Hersbach, H.; Bell, B.; Berrisford, P.; Hirahara, S.; Horanyi, A.; Muñoz-Sabater, J.; Nicolas, J.; Peubey, C.; Radu, R.; Schepers, D.; et al. The ERA5 global reanalysis. *Q. J. R. Meteorol. Soc.* **2020**, *146*, 1999–2049. [CrossRef]
46. Vitolo, C.; Di Giuseppe, F.; Krzeminski, B.; San-Miguel-Ayanz, J. A 1980–2018 global fire danger re-analysis dataset for the Canadian Fire Weather Indices. *Sci. Data* **2019**, *6*, 190032. [CrossRef]
47. LANDFIRE. *LANDFIRE: 40 Scott and Burgan Fire Behavior Fuel Models*; U.S. Department of Agriculture and U.S. Department of Interior: Washington, DC, USA, 2016.
48. Kennedy, M.C.; Johnson, M.C.; Fallon, K.; Mayer, D. How big is enough? Vegetation structure impacts effective fuel treatment width and forest resiliency. *Ecosphere* **2019**, *10*, e02573. [CrossRef]
49. Moghaddas, J.J.; Collins, B.M.; Menning, K.; Moghaddas, E.E.; Stephens, S.L. Fuel treatment effects on modeled landscape-level fire behavior in the northern Sierra Nevada. *Can. J. For. Res.* **2010**, *40*, 1751–1765. [CrossRef]
50. Finney, M.A. Design of regular landscape fuel treatment patterns for modifying fire growth and behavior. *For. Sci.* **2001**, *47*, 219–228.
51. CAL FIRE. CAL FIRE Fuel Breaks and Use during Fire Suppression: Fuel Break Design, Construction, Environmental Protection and Case Studies in Community Protection. 2019. Available online: https://www.fire.ca.gov/media/5585/fuel_break_case_studies_03212019.pdf (accessed on 24 November 2021).
52. Butte County District Attorney. The Camp Fire Public Report, a Summary of the Camp Fire Investigation. Oroville, CA. 2020. Available online: <https://www.buttecounty.net/Portals/30/CFReport/PGE-THE-CAMP-FIRE-PUBLIC-REPORT.pdf?ver=2020-06-15-190515-977> (accessed on 24 November 2021).
53. Cruz, M.G.; Alexander, M.E.; Fernandes, P.M.; Kilinc, M.; Sil, A. Evaluating the 10% wind speed rule of thumb for estimating a wildfire’s forward rate of spread against an extensive independent set of observations. *Environ. Model. Softw.* **2020**, *133*, 104818. [CrossRef]
54. Stocks, B.J.; Alexander, M.E.; Wotton, B.M.; Stefrer, C.N.; Flannigan, M.D.; Taylor, S.W.; Lavoie, N.; Mason, J.A.; Hartley, G.R.; Maffey, M.E.; et al. Crown fire behaviour in a northern jack pine–black spruce forest. *Can. J. For. Res.* **2004**, *34*, 1548–1560. [CrossRef]

55. Overholt, K.J.; Cabrera, J.; Kurzawski, A.; Koopersmith, M.; Ezekoye, O.A. Characterization of Fuel Properties and Fire Spread Rates for Little Bluestem Grass. *Fire Technol.* **2014**, *50*, 9–38. [[CrossRef](#)]
56. Stechishen, E.; Little, E.C.; Hobbs, M.W.; Murray, W.G. *Productivity of Skimmer Air Tankers*; Information Report PI-X-15; Environment Canada, Canadian Forestry Service, Petawawa National Forestry Institute: Chalk River, ON, Canada, 1982; pp. 1–16.
57. Page, W.G.; Wagenbrenner, N.S.; Butler, B.W.; Blunck, D.L. An analysis of spotting distances during the 2017 fire season in the Northern Rockies, USA. *Can. J. For. Res.* **2018**, *49*, 317–325. [[CrossRef](#)]
58. Storey, M.A.; Price, O.F.; Almeida, M.; Ribeiro, C.; Bradstock, R.A.; Sharples, J.J. Experiments on the influence of spot fire and topography interaction on fire rate of spread. *PLoS ONE* **2021**, *16*, e0245132. [[CrossRef](#)]
59. Potter, B.E. Atmospheric interactions with wildland fire behaviour-II. Plume and vortex dynamics. *Int. J. Wildland Fire* **2012**, *21*, 802–817. [[CrossRef](#)]
60. Greenbelt Alliance. The Critical Role of Greenbelts in Wildfire Resilience. Available online: <https://www.greenbelt.org/wp-content/uploads/edd/2021/06/The-Critical-Role-of-Greenbelts-in-Wildfire-Resilience.pdf> (accessed on 24 November 2021).
61. Green, L.R. *Fuelbreaks and Other Fuel Modification for Wildland Fire Control*; Agricultural Handbook No. 499. 79; US Department of Agriculture, Forest Service: Washington, DC, USA, 1977; p. 499.
62. Wong, S.; Broader, J.; Shaheen, S. *Review of California Wildfire Evacuations from 2017 to 2019*; Institute of Transportation Studies, Research Reports, Working Papers, Proceedings; University of California, Berkeley: Berkeley, CA, USA, 2020.
63. California Governor. Newsom Administration Awards Nearly \$138 Million in Fire Prevention Grants to Build Resilience in Local Communities. 2021. Available online: <https://www.gov.ca.gov/2021/09/15/newsom-administration-awards-nearly-138-million-in-fire-prevention-grants-to-build-resilience-in-local-communities/> (accessed on 24 November 2021).

Supporting Information

The grass fuel properties used for the fuel break

Table S1. The specifications of the M-1 (mixed wood) and O-1b (grass) fuel types used in the Prometheus model.

M-1		O-1b (for landscape)		O-1b (for WUI fuel break)	
Tree height	13 m	degree of curing	60%	degree of curing	10/30/50%
Canopy base height	6 m	fuel load	3.5 t ha ⁻¹	fuel load	1.7/3.5/7 t ha ⁻¹
Crown fuel load	0.8 kg m ⁻²				
Foliar moisture content	120%				

WRF model verification

Slightly underestimated 2-m air temperature and overestimated 2-m RH values in the WRF forecast model for the Jarbo Gap RAWS location in our study are in good agreement with the WRF simulation with 444 m horizontal grid spacing presented in [28].

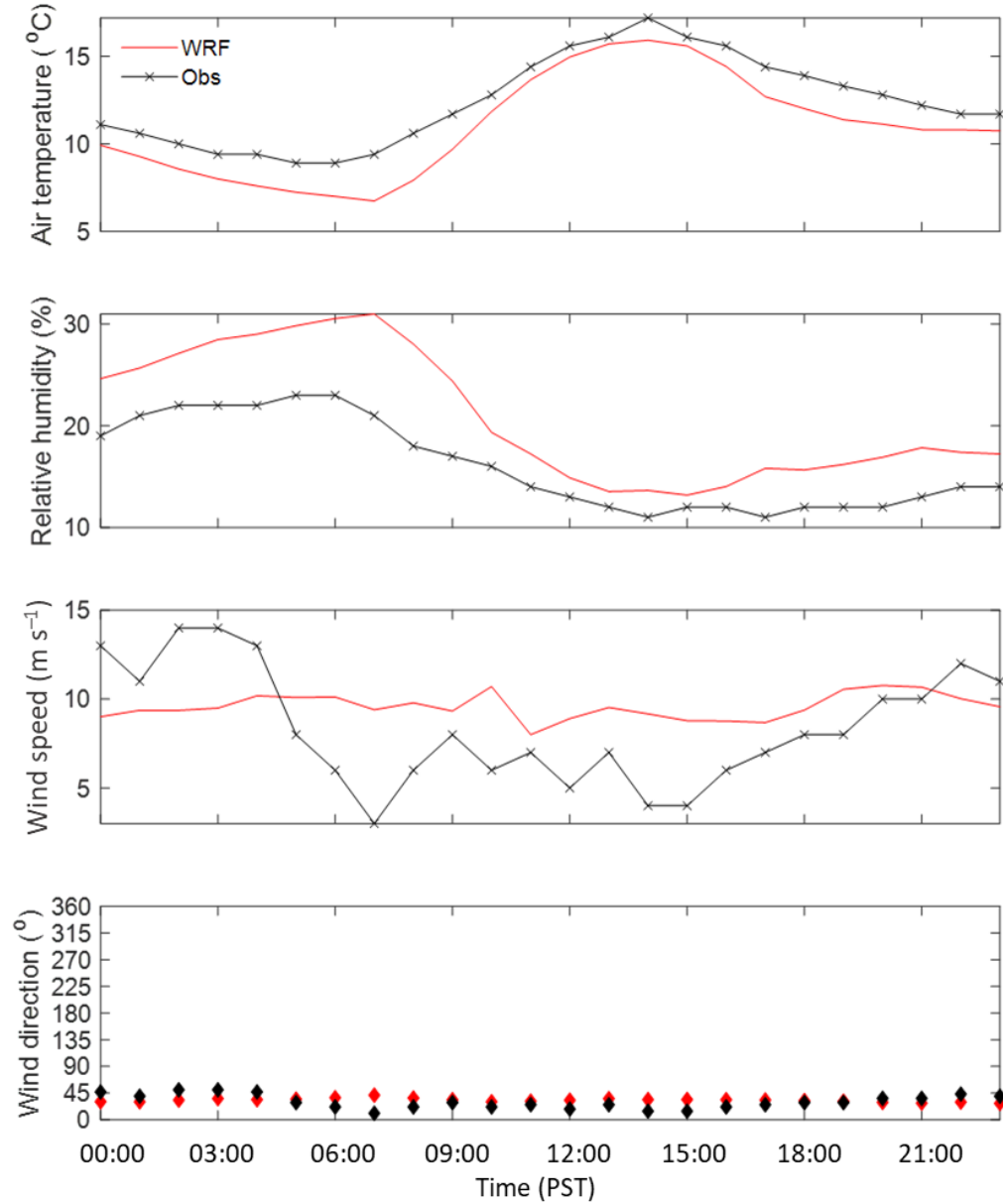


Figure S1. Observed weather data at Jarbo Gap weather station vs. WRF output at the nearest grid point for a sample diurnal cycle. The dashed red vertical line indicates approximate fire ignition time.

Vertical wind profiles of the WRF simulation near the ignition point

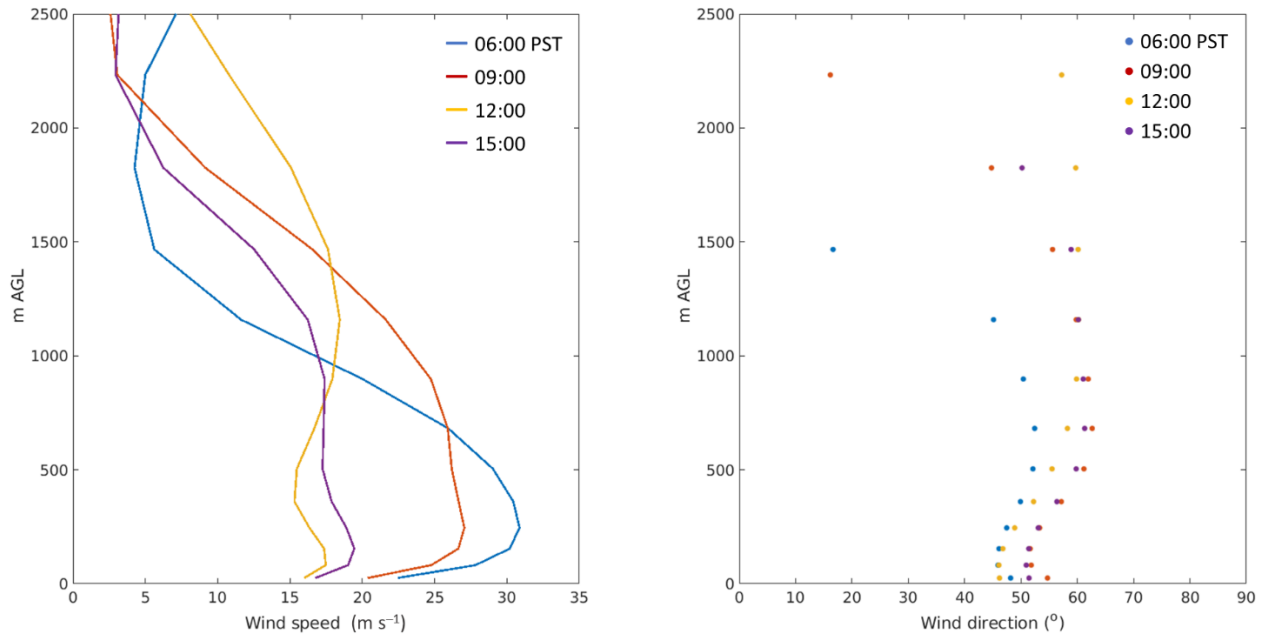


Figure S2. WRF simulation of vertical profiles of (left) wind speeds and (right) wind directions at the upwind weather stream location between 06:00 and 15:00 PST on 8 Nov 2018.

Impact of non-burnable housing structures on fire spread simulations

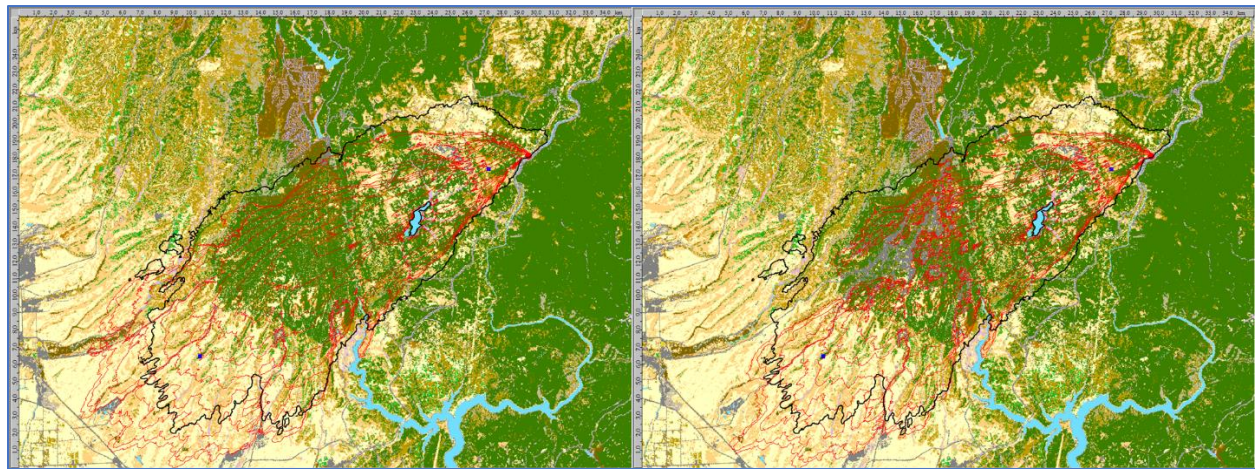


Figure S3. Fire growth simulations (red contour lines) using a fuel patch that replaced non-burnable fuel type (grey color) with a M-1 (90% percent conifer value) fuel type (left) and without a fuel patch (right). The solid black outline shows the observed burned perimeter at 18:00 PST.

Dominant fuel types inside the observed burn perimeter

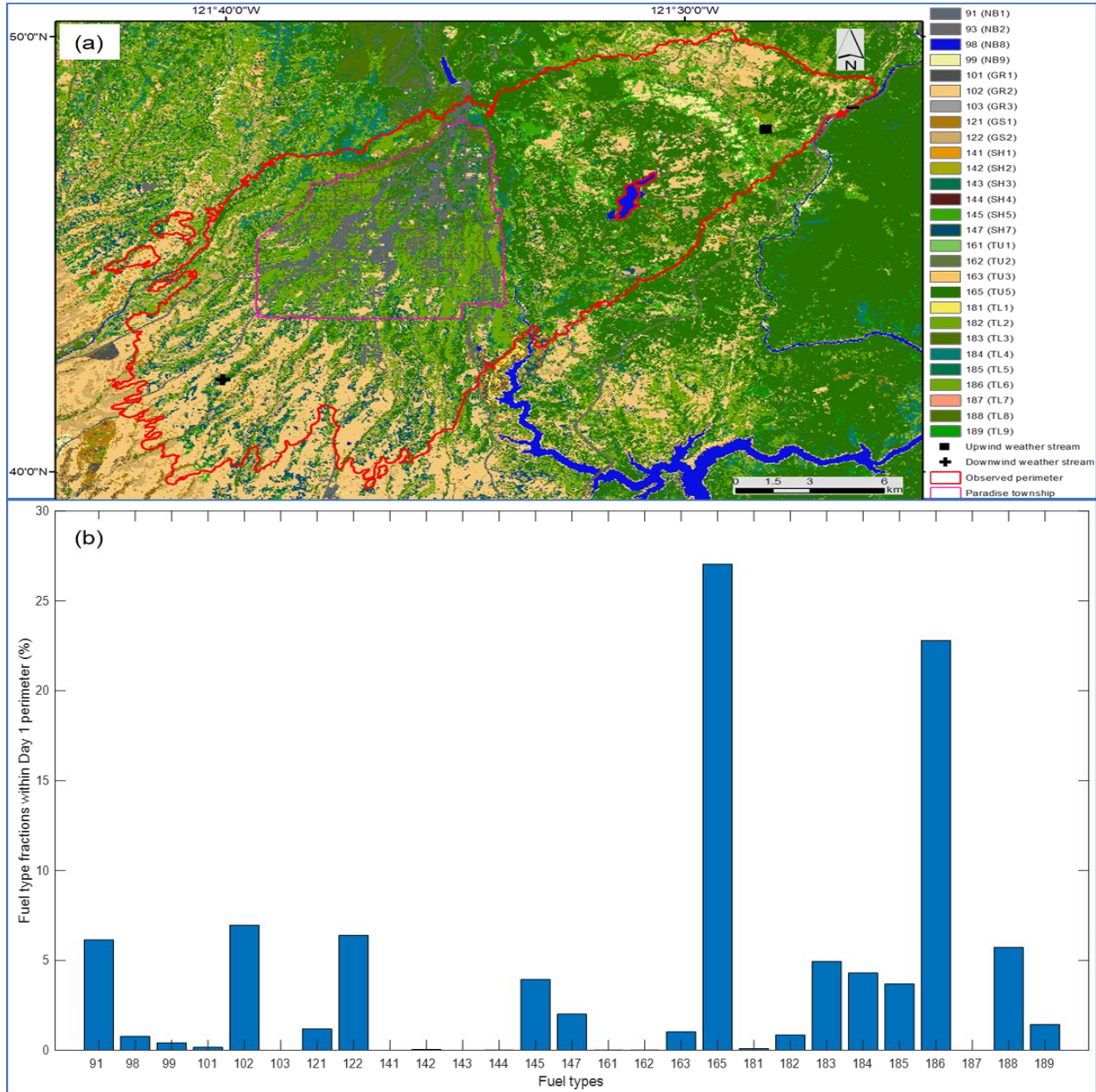


Figure S4. (a) Vegetation map of the study area created using Scott and Burgan fuel model data downloaded from the LANDFIRE website. (b) a fuel distribution inside the observed burn perimeter (red contour outline in (a)).

Impact of FFMC on fire spread

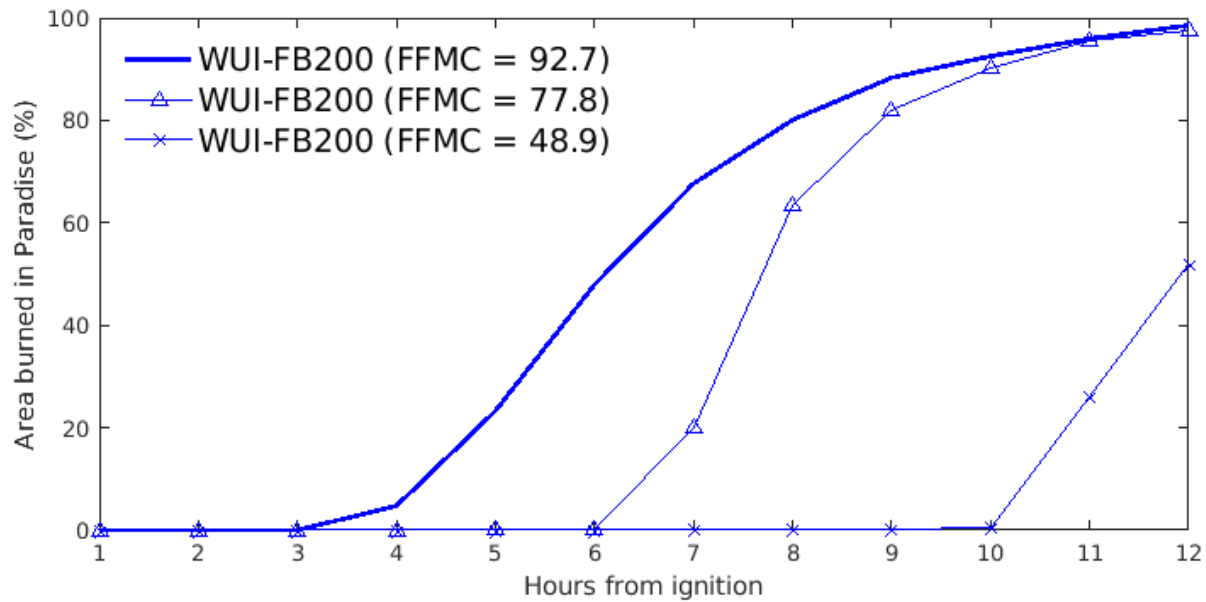


Figure S5. Percent of area burned in Paradise (inside the magenta polygon in Figure 1) vs. time after ignition in hours for the 200 m WUI fuel break runs with different FFMC values.